

The azimuthal magnetorotational instability (AMRI)

G. Rüdiger¹, M. Gellert¹, M. Schultz¹, R. Hollerbach^{2,3}, F. Stefani⁴

¹*Leibniz-Institut für Astrophysik Potsdam, An der Sternwarte 16, 14482 Potsdam, Germany*

²*ETH Zürich, Institut für Geophysik, Sonneggstr 5, 8092 Zürich, Switzerland*

³*University of Leeds, School of Mathematics, Woodhouse Lane, Leeds, LS2 9JT, UK*

⁴*Helmholtz-Zentrum Dresden-Rossendorf, POB 51 01 19, 01314 Dresden, Germany*

Accepted . Received ; in original form

ABSTRACT

We consider the interaction of differential rotation and toroidal fields that are current-free in the gap between two corotating axially unbounded cylinders. It is shown that nonaxisymmetric perturbations are unstable if the rotation rate and Alfvén frequency of the field are of the same order almost independent of the magnetic Prandtl number Pm . For the very steep rotation law $\Omega \propto R^{-2}$ (the Rayleigh limit) this Azimuthal MagnetoRotational Instability (AMRI) scales with the ordinary Reynolds number and the Hartmann number, which allows a laboratory experiment with liquid metals like sodium or gallium in a Taylor-Couette container. The growth rate of AMRI scales with Ω^2 in the low-conductivity limit and with Ω in the high-conductivity limit. For the weakly nonlinear system the numerical values of the kinetic energy and the magnetic energy are derived for magnetic Prandtl numbers between 0.05 and unity. We find that the magnetic energy scales with the magnetic Reynolds number Rm , while the kinetic energy scales with $\text{Rm}/\sqrt{\text{Pm}}$. The resulting turbulent Schmidt number as the ratio of the diffusion coefficients of angular momentum and a passive scalar (such as lithium) is of order 20 for $\text{Pm} = 1$, but for small Pm drops to order unity. Hence, in a stellar core with fossil fields and steep rotation law the transport of angular momentum by AMRI is always accompanied by an intense mixing of the plasma, until the rotation becomes rigid.

Key words: magnetohydrodynamics (MHD) – instabilities – stars: magnetic fields – stars: interiors.

1 INTRODUCTION

A hydrodynamically stable rotation law may become unstable under the presence of a sufficiently strong uniform axial field. For this so-called magnetorotational instability (MRI) the axial field gives the catalyst which makes the rotation law unstable without any modification of the uniform field (Velikhov 1959). Of course, by this mechanism a protoplanetary disk with a Keplerian rotation law should also become unstable if it is not too cold – or (almost) equivalently – if the field is strong enough. For an estimation of the critical magnetic field strength it is enough to use the condition $S \gtrsim 1$, where the Lundquist number

$$S = \frac{B_z H}{\sqrt{\mu_0 \rho} \eta}, \quad (1)$$

with B_z the amplitude of the axial field, H the semi-thickness of the disk, and η the microscopic magnetic diffusivity. Plotted in the S - Rm plane, with

$$\text{Rm} = \frac{\Omega H^2}{\eta} \quad (2)$$

as the magnetic Reynolds number, and for small magnetic Prandtl number $\text{Pm} = \nu/\eta$, the viscosity hardly influences the instability map. At a distance of 1 AU from a central mass with $1 M_\odot$ the disk thickness is about 3%, the density ρ of the gas 10^{-10} g/cm^3 , and $\eta \simeq 4 \cdot 10^{15} \text{ cm}^2/\text{s}$ (because of the low temperature of the gas). Hence, the surprisingly high value of 0.1 gauss is obtained for the minimum B_z .

In order to excite nonaxisymmetric MRI modes one needs even higher magnetic fields. Kitchatinov & Rüdiger (2010) showed in a linear theory that nonaxisymmetric modes only arise if $\Omega_A \gtrsim 0.05 \Omega$, with the Alfvén frequency $\Omega_A = B_z / \sqrt{\mu_0 \rho} H$. For $\Omega = 2 \cdot 10^{-7}$ at 1 AU this condition is fulfilled for $B_z \gtrsim 0.3$ gauss. Such strong fields at this distance cannot be due to a stellar dipole field in the center. On the other hand, one should mention that the fossil magnetic fields found in meteorites are of just this order. One solution of this dilemma is to consider toroidal fields, which by the stretching action of differential rotation may often exceed the values of the poloidal field. For protoplanetary disks, however, the magnetic Reynolds number Rm only reaches

values of about 50, so that the resulting toroidal field does *not* dominate the original B_z .

The same is true for galaxies when the interstellar turbulence is driven by SN-explosions. The resulting magnetic Reynolds number is then also of order 10–100, so that the induced toroidal field does not dominate the poloidal one – as observed.

A very different situation holds for the radiative cores of rotating stars. Due to the high conductivity of the hot plasma the magnetic Reynolds number is so large that even very slight differential rotation will produce toroidal fields which clearly dominate the fossil poloidal fields. It should then be sufficient to consider the stability of only the strong toroidal field under the presence of differential rotation. In the present paper we shall always apply a rotation law close to the profile of uniform specific angular momentum, i.e. $\Omega \propto R^{-2}$. This rather steep profile is just beyond the regime of hydrodynamic centrifugal instability, also in spherical systems (see Rüdiger & Kitchatinov 1996).

There are basic stability conditions in cylindrical geometry. A flow is stable against axisymmetric perturbations if

$$\frac{d}{dR} (R^2 \Omega)^2 > \frac{R^4}{\mu_0 \rho} \frac{d}{dR} \frac{B_\phi^2}{R^2} \quad (3)$$

(Michael 1954). This condition turns into the well-known Rayleigh criterion for both $B_\phi = 0$ and $B_\phi \propto R$. The latter case means that an axial uniform electric current does not suppress Taylor vortices, which are due to too steep rotation profiles. Hence, rotation laws which are steeper than $\Omega \propto R^{-2}$ will always excite axisymmetric rolls, even under the presence of very strong toroidal fields with $B_\phi \propto R$. On the other hand, any unstable Ω -profiles can be stabilized with a toroidal field of sufficiently large amplitude and suitable geometry.

If nonaxisymmetric modes are considered then the necessary and sufficient condition for stability becomes

$$\frac{d}{dR} (R B_\phi^2) < 0 \quad (4)$$

(Tayler 1957, 1973, Vandakurov 1972), at least in the absence of rotation. The fully general formulation including rotation is not known. Two questions immediately arise: i) is the field corresponding to a uniform current ($B_\phi \propto R$) really unstable, and ii) does the current-free field $B_\phi \sim R^{-1}$ become unstable under the presence of (differential) rotation? Both questions can be answered. In the first case the resulting instability is called the Tayler instability (TI), and in the second case, where fields and rotation profiles that would each be stable on their own interact to yield instability, the result is called the Azimuthal MagnetoRotational Instability (AMRI). Whereas the energy for the TI comes from the electric current, the energy source for AMRI is entirely from the differential rotation, and AMRI can only saturate at the expense of the rotational shear by producing high values of ‘eddy’ viscosity. This could therefore justify the high values of ‘artificial’ viscosity which Eggenberger, Montalbán & Miglio (2012) introduced to explain the slow rotation of the stellar cores after the collapse towards their red giant stage.

It is possible to demonstrate the mechanism which leads to AMRI with a simple dispersion relation for the stability

of *nonaxisymmetric* perturbations in the form $\exp(\gamma t + k z + m \phi)$ with $\Re(\gamma)$ as the growth rate. It is enough to apply the case with $\text{Pm} \rightarrow 0$ and $\Omega \propto 1/R^2$ (the Rayleigh limit) to the expressions given by Kirillov, Stefani & Fukumoto (2012) for nonaxisymmetric perturbations, which leads to the dispersion relation of second order

$$\text{Re}^{*2} \hat{\omega}^2 + \text{Re}^* (a_3 + i b_3) \hat{\omega} + a_4 + i b_4 = 0. \quad (5)$$

Here we have used the quantity $\hat{\omega} = \gamma / \sqrt{\text{Pm} \cdot \text{Re}}$ with $\text{Re} = \Omega / \nu k^2$ as the growth rate in units of the angular velocity of rotation. The imaginary part of $\hat{\omega}$ describes an azimuthal drift of the nonaxisymmetric pattern (see below).

The coefficients a and b are

$$\begin{aligned} a_3 &= 2(1 + (2 + m^{*2} \text{Ha}^*)), & b_3 &= 2m^* \text{Re}^* \\ a_4 &= 1 + (4 + 2m^{*2}) \text{Ha}^{*2} + m^{*4} \text{Ha}^{*4} - m^{*2} \text{Re}^{*2} \\ b_4 &= 2\text{Re}^* m^* (1 + m^{*2} \text{Ha}^{*2}) \end{aligned} \quad (6)$$

with the abbreviations

$$\text{Re}^* = \alpha \text{Re}, \quad \text{Ha}^* = \frac{\alpha}{kR} \text{Ha}, \quad m^* = \frac{m}{\alpha}, \quad (7)$$

where $\alpha = k_z/k$ and $\text{Ha} = B_\phi/k \cdot \sqrt{\mu_0 \rho \nu \eta}$.

The formal solution of (5) for marginal instability leads to the two conditions

$$\hat{\omega}_{\text{dr}} = -\frac{b_4}{\text{Re}^* a_3}, \quad a_3(a_3 a_4 + b_3 b_4) = b_4^2. \quad (8)$$

The first of these relations gives the negative drift rate in units of the basic rotation, i.e.

$$\frac{\omega_{\text{dr}}}{\Omega} = -\frac{m^* (1 + m^{*2} \text{Ha}^{*2})}{1 + (2 + m^{*2}) \text{Ha}^{*2}}. \quad (9)$$

The observable drift in the laboratory system, $d\phi/dt = -\omega_{\text{dr}}/m$, is thus positive (in the rotation direction) and with $d\phi/dt \leq k\Omega/k_z$ it is (for large Hartmann numbers) independent of the magnetic field, and also of the sign of the mode number m .

The second condition in (8) leads to

$$\text{Re}^* \simeq \frac{m^{*3} \text{Ha}^{*2}}{2}, \quad (10)$$

the latter relation holding for strong fields. For medium magnetic field the relation changes to a linear one. Axisymmetric solutions do not exist. It is clear also that the mode with $m = 1$ is most easily excited:

$$\text{Re} \simeq \frac{1}{2} \frac{\text{Ha}^2}{k_z^2 R^2}, \quad (11)$$

valid again for large Ha . Solutions with large axial wave number – representing oblate cells – need much slower rotation to be excited.

For the Elsasser number $\Lambda = B_\phi^2 / \mu_0 \rho \eta \Omega$ we obtain the relation

$$\Lambda \simeq 2(k_z R)^2, \quad (12)$$

where the influence of the microscopic viscosity completely disappears.

With view on the experimental demonstration of AMRI we consider a Taylor-Couette set-up with two corotating cylinders of nearly perfectly conducting material. The cylinders confine an incompressible, conducting fluid under the presence of a toroidal magnetic field. It is clear that the radial profiles of the rotating flow and the field between the cylinders are

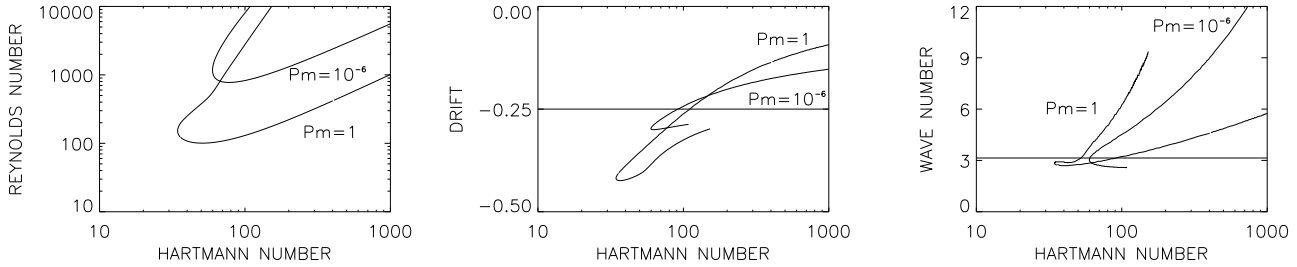


Figure 1. The AMRI at the Rayleigh limit, $\mu_\Omega = 0.25$, for the two magnetic Prandtl numbers $Pm = 10^{-6}$ and $Pm = 1$. Left: the instability map, middle: the azimuthal drift of the solutions normalized with Ω_{in} , right: the axial wave number multiplied with the gap width.

$$U_\phi = R\Omega = a_\Omega R + \frac{b_\Omega}{R}, \quad B_\phi = a_B R + \frac{B_b}{R}. \quad (13)$$

Let the ratio of the rotation rates of the cylinders be $\mu_\Omega = \Omega_{out}/\Omega_{in}$ and a similar expression for the field amplitudes, i.e.

$$\mu_B = \frac{B_{out}}{B_{in}}. \quad (14)$$

The ratio of the cylinder radii is $r_{in} = R_{in}/R_{out}$, where we will fix $r_{in} = 0.5$. For such a container $\mu_\Omega = 0.25$ describes the Rayleigh limit for which $R^2\Omega \simeq \text{const}$ (‘shellular’ rotation, $a_\Omega = 0$ in Eq. (13)), while $\mu_\Omega = 0.5$ describes the quasi-galactic rotation law $U_\phi \simeq \text{const}$. Only these two rotation laws will be considered in detail here.

For the magnetic field the expressions in (13) also contain two extrema. With $b_B = 0$ the toroidal field is due to a homogeneous current inside the fluid. For $r_{in} = 0.5$ the corresponding value is $\mu_B = 2$. Such fields are unstable according to the criterion (4) against nonaxisymmetric perturbations. The existence of this kink-type ‘Taylor’ instability has recently been shown in the laboratory (Seilmayer et al. 2012, Rüdiger et al. 2012).

The equations and boundary conditions are given by Rüdiger et al. (2007) and will not be repeated here. We imagine the cylinders, which are unbounded in the axial direction, to be made of a perfectly conducting material. AMRI in the described container appears for $\mu_B = 0.5$. The electric current only flows within the inner cylinder; no background electric current flows through the fluid between the cylinders.

For the rotation law with $\mu_\Omega = 0.25$ (the Rayleigh limit) the plots in Fig. 1 demonstrate the characteristic values of the solutions. The critical Reynolds numbers (left), drift rates (middle) and wave numbers (right) are given for the magnetic Prandtl numbers 10^{-6} and 1, which differ by many orders of magnitudes. The differences of the characteristic values given in Fig. 1, however, remain very small. The AMRI at the Rayleigh limit can be more easily excited for $Pm = 1$ than for $Pm \rightarrow 0$, but the effect is weak compared with the variation of the magnetic Prandtl number. Obviously, the AMRI close to the Rayleigh limit scales for various Pm with the Reynolds number and with the Hartmann number (Hollerbach et al. 2010). As an immediate consequence, the existence of the AMRI can be proven by laboratory experiments with liquid metals with their very low values of Pm – just as the helical MRI (Stefani et al. 2009), but in strong contrast to the standard MRI which is

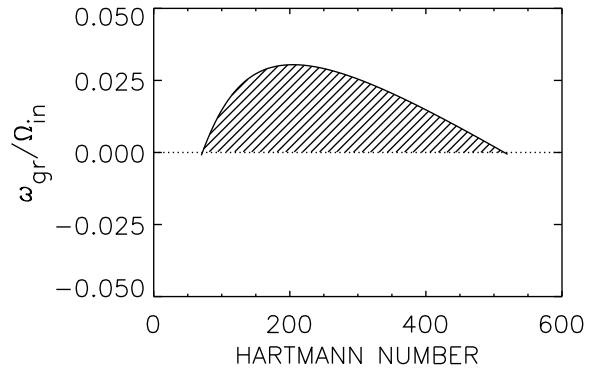


Figure 2. The normalized growth rate $\omega_{gr} = \Im(\omega)/\Omega_{in}$ as function of the toroidal background field. $m = \pm 1$. $\mu_\Omega = 0.25$, $Re = 3000$, $Pm = 10^{-6}$.

much harder to achieve (Rüdiger & Hollerbach 2004). The results obtained with materials with low Pm are also representative of materials with Pm of order unity. Typical values for such possible experiments are $Re \simeq 1000$ and $Ha \simeq 100$.

The meaning of the marginal instability curves is explained by the growth rates, given in Fig. 2 for a fixed Reynolds number $Re = 3000$. The growth rate is positive between the two critical values, which in Fig. 1 (left) enclose a region of instability. The maximum growth rate of 0.02 lies between the two limiting Hartmann numbers, and implies a growth time of about 7 rotation times. Compared with the standard MRI the AMRI is slower.

As the left-hand plot of Fig. 1 also shows, the AMRI instability domain is always limited by two values of the Reynolds number or two values of the Hartmann number. For fixed rotation rate the magnetic field can be too weak or too strong, and conversely for fixed magnetic field the rotation can be too slow or too fast.

The azimuthal drift rates (Fig. 1, middle) are always negative, hence the pattern of the instability wave drifts in the direction of the basic rotation (see above). A typical value of the drift (normalized with Ω_{in}) for small Pm is 0.25 (marked in the plot), which hardly depends on the Hartmann number. For both the Rayleigh limit and the rotation ratio $\mu_\Omega = 0.25$ the pattern essentially corotates with the outer cylinder. For stronger fields the drift is slightly slower.

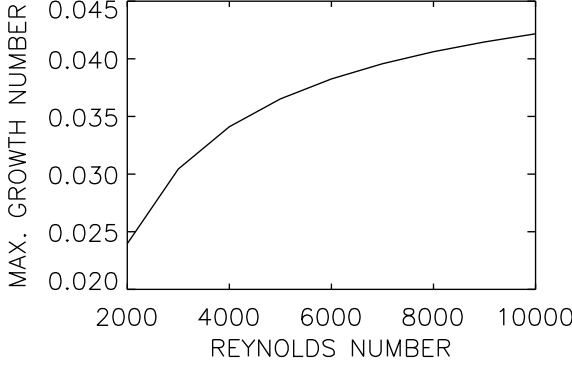


Figure 3. The *maximal* normalized growth rate as a function of the Reynolds number for $\mu_\Omega = 0.25$. The Hartmann numbers which correspond to the maxima vary from about 200 to about 500 from the left to the right axis of the plot. $\text{Pm} = 10^{-6}$.

The right-hand plot in Fig. 1 gives the axial wave numbers normalized with the gap width $d = R_{\text{out}} - R_{\text{in}}$. A wave number of π (marked) describes a cell with a circular geometry in the radial and the vertical coordinates. Precisely this cell form exists for the instability at the weak-field end of the instability domain. For stronger fields the cells become more oblate (not prolate!) but this is only true for the lower branches of the instability map. Along the upper branches the cells preserve their circular shape.

One must ask how the growth rate behaves for increasingly rapid rotation. To answer this question one must determine the maxima known from Fig. 2 for increasing Reynolds numbers. The results given in Fig. 3 clearly show the saturation of $\omega_{\text{gr}} = \Im(\omega)/\Omega_{\text{in}}$. The maximum growth rate for very rapid rotation is $0.045 \Omega_{\text{in}}$, so that the shortest growth time of AMRI at the Rayleigh limit is 3.5 rotation times.

2 QUASI-GALACTIC ROTATION

For the quasi-galactic rotation law with $\mu_\Omega = 0.5$, Fig. 4 shows the domain of instability in the S - Rm plane, for various magnetic Prandtl numbers. It is obvious that for $\text{Pm} \lesssim 1$ the values scale with the magnetic Reynolds number Rm and the Lundquist number S , i.e.

$$\text{Rm} = \frac{\Omega_{\text{in}} d^2}{\eta}, \quad S = \frac{B_{\text{in}} d}{\sqrt{\mu_0 \rho} \eta}. \quad (15)$$

The unstable domain in the plane again has the characteristic form of tilted cones, so that minimal and maximal values of both S and Rm always exist for the onset of the instability. Hence, both the magnetic field and the rotation rate can be too weak or too strong for AMRI. One also finds that the instability curves for $\text{Pm} \rightarrow 0$ converge in the S - Rm plane. For all Pm the ratio Ω_{A}/Ω lies between a low-field limit and a high-field limit, e.g., for $\text{Pm} = 1$,

$$0.3 \lesssim \frac{\Omega_{\text{A}}}{\Omega} \lesssim 1. \quad (16)$$

It is thus clear that for AMRI the Alfvén frequency of the toroidal magnetic field and the rotation rate must be of the same order. If the toroidal field is produced by differential

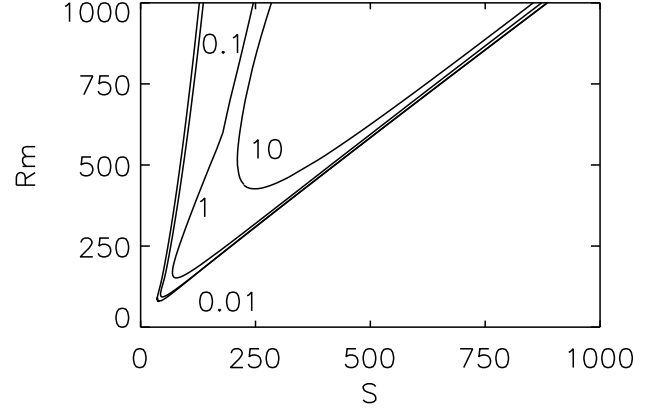


Figure 4. The instability map for the quasi-galactic rotation law $\mu_\Omega = 0.5$ in the S - Rm -plane. $m = \pm 1$. The curves are marked with their values of the magnetic Prandtl number.

rotation acting on a poloidal fossil field, then the low-field limit in Eq. (16) plays the role of the onset condition for the axisymmetric instability.

For given Rm and Pm the growth rate has been calculated between the two limiting values S where it vanishes; it is maximal somewhere between the two limits. In Figs. 5 the ratio $\omega_{\text{gr}}/\Omega_{\text{in}}$ is plotted for various Rm and Pm . For fixed Pm one finds a quasi-linear relation

$$\frac{\omega_{\text{gr}}}{\Omega_{\text{in}}} \simeq \varepsilon_{\text{gr}} \text{Rm} \quad (17)$$

or

$$\omega_{\text{gr}} \simeq \varepsilon_{\text{gr}} \frac{\Omega_{\text{in}}^2}{\omega_\eta} \quad (18)$$

with ε_{gr} of order 10^{-4} . It varies from $1.5 \cdot 10^{-4}$ for $\text{Pm} = 1$ to $2.1 \cdot 10^{-4}$ for $\text{Pm} = 0.01$, which suggests a very weak dependence of the growth rate ω_{gr} on Pm . Hence, the growth time in units of the rotation time is $\tau_{\text{gr}}/\tau_{\text{rot}} \simeq 10^3/\text{Rm}$ for small Rm . For smaller Rm the AMRI is rather slow, but the linear relation (17) can only hold for small Rm . Figure 5 shows that the growth rate slowly grows for smaller Pm but this effect is rather weak.

The saturation of the normalized growth rate for $\text{Pm} = 1$ is demonstrated by Fig. 6. For sufficiently rapid rotation the dependence of $\hat{\omega}_{\text{gr}}$ on the value of Rm disappears, so that always $\Im(\omega)/\Omega_{\text{in}} \leq 0.14$. The growth time, therefore, for the instability of the considered rotation law and for $\text{Pm} = 1$ can never be shorter than one rotation time.

3 DESIGN OF AN EXPERIMENT

With the given data it is easy to design an experiment for the realization of AMRI in the laboratory. For experiments on magnetically induced instabilities of the differential rotation beyond the Rayleigh limit it is natural to work with a Taylor-Couette container with a rotation law of $\mu_\Omega = 0.26$, which by itself would be hydrodynamically stable. For $\text{Re} = 3000$ Fig. 7 shows that the limit of marginal instability is reached for a Hartmann number of 85. Note that the instability region

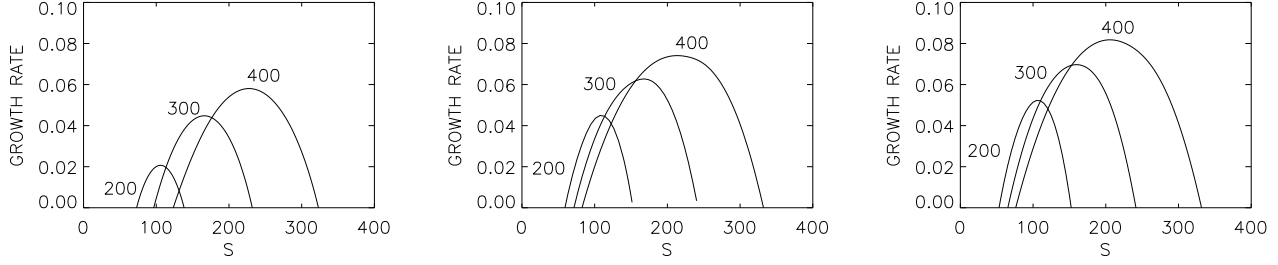


Figure 5. The normalized growth rate $\hat{\omega}_{\text{gr}} = \Im(\omega)/\Omega_{\text{in}}$ as a function of the toroidal background field. The curves are marked with their values of the magnetic Reynolds number. $m = \pm 1$, $\mu_{\Omega} = 0.5$, $\text{Pm} = 1$ (left), $\text{Pm} = 0.1$ (middle), $\text{Pm} = 0.01$ (right).

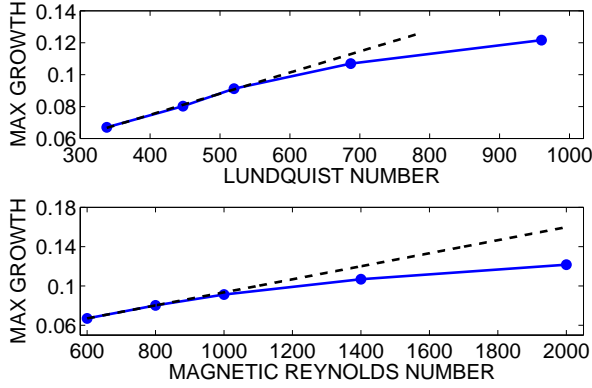


Figure 6. The normalized growth rate $\hat{\omega}_{\text{gr}} = \Im(\omega)/\Omega_{\text{in}}$ for $\mu_{\Omega} = 0.5$, optimized in the tilted instability cone for $\text{Pm} = 1$ as a function of S (top) or Rm (bottom).

is slightly smaller than for the rotation law with $\mu_{\Omega} = 0.25$, which is understandable as the energy for AMRI is completely provided by the energy of the shear.

The relation $I_{\text{axis}} = 5R_{\text{in}}B_{\text{in}}$ connects the toroidal field amplitude B_{in} at R_{in} with the axial current inside the inner cylinder. I , R and B must be measured in ampere, cm and gauss. Hence,

$$\text{Ha} = \frac{1}{5} \frac{I_{\text{axis}}}{\sqrt{\mu_0 \rho \nu \eta}}. \quad (19)$$

The radial size of the container does not occur in this relation between the Hartmann number and the current amplitude. For the gallium alloy GaInSn the magnetic Prandtl number is $1.4 \cdot 10^{-6}$ and the value of the square root in (19) is 25.6. The resulting electric current for marginal instability is 10.9 kA.

For a container with (say) $R_{\text{in}} = 4$ cm and with the viscosity of GaInSn ($\nu = 3.4 \cdot 10^{-3}$ cm²/s) the Reynolds number $\text{Re} = 3000$ requires a rotation rate of the inner cylinder of only 0.1 Hz. Figure 8 shows that for the weakest fields the cell structure of the nonaxisymmetric pattern is circular and that the pattern nearly drifts with the same rotation rate as the outer cylinder. Both properties are very characteristic for the instability close to the marginal limit for weak magnetic fields – independent of the steepness μ_{Ω} of the rotation law. Such an experiment is currently operating at the Helmholtz-Zentrum Dresden-Rossendorf. The results will be presented in a separate paper.

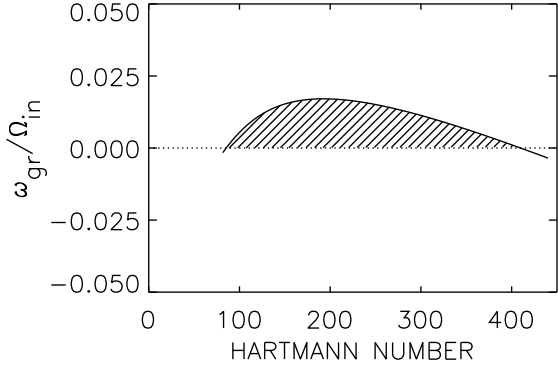


Figure 7. The normalized growth rate for an experiment with $\mu_{\Omega} = 0.26$ as a function of the toroidal background field. $m = \pm 1$, $\text{Re} = 3000$, $\text{Pm} = 10^{-6}$. There are no visible differences to the results for $\text{Pm} = 0$.

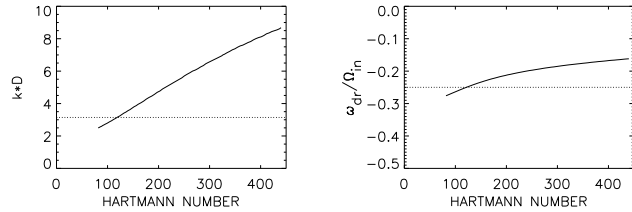


Figure 8. The normalized wave number (left) and drift rate (right) for fixed Reynolds number $\text{Re} = 3000$. The dotted lines give the wave number of π for a circular cell structure (left) and the drift rate of -0.25 for corotation of the pattern with the outer cylinder (right). $m = \pm 1$, $\mu_{\Omega} = 0.26$, $\text{Pm} = 10^{-6}$.

4 KINETIC AND MAGNETIC ENERGY OF THE INSTABILITY

We have seen that the modes for $m = 1$ and $m = -1$, corresponding to left and right spiraling modes (Hollerbach et al. 2010) are fully degenerate, i.e. they are excited at the same eigenvalues and possess the same wave numbers and drift rates. For the following nonlinear calculations the spectral cylindrical MHD code of Gellert, Rüdiger & Fournier (2007) is used. The solution is expanded in azimuthal Fourier modes. The resulting meridional problems are solved with a

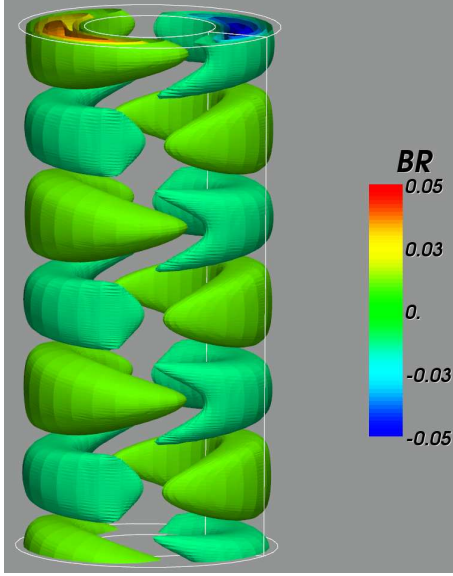


Figure 9. The nonlinear instability pattern of AMRI is a combination of the modes $m = \pm 1$ which drifts with a common drift rate. There are seven cells along the axial direction with the aspect ratio $\Gamma = 8$. The cells are thus slightly elongated. $Re = 500$, $Ha = 80$, $\mu_\Omega = 0.26$, $Pm = 0.1$.

Legendre spectral element method after Deville, Fischer & Mund (2002). The code, however, is only able to solve equations with a minimum magnetic Prandtl number of 0.01. Fig. 9 shows the structure of the resulting wave, which consists of both $m = \pm 1$ components, and drifts together with the outer cylinder. The almost circular meridional cell structure also confirms the results of the linear theory. There are seven cells along the vertical axis with its eight length units.

Besides the geometric structure, the nonlinear code also provides the behavior of the equilibrated energies. The questions are how strong the magnetic energy is (i) in units of the kinetic energy, and (ii) in units of the energy of the toroidal background field. The maximal amplitude of the radial field component in units of B_{in} in Fig. 9 is rather small. This fact, however, is only due to the rather slow rotation of this example.

Figure 10 displays the energies of several instability models for magnetic Prandtl numbers between 0.05 and 1.0. Both the magnetic and the kinetic energy are integrated and normalized with the energy of the toroidal background field. All energies are integrals over the entire container. The first finding concerns the quantity $q = \langle b^2 \rangle / \langle B_{in}^2 \rangle$, which for driven turbulence in the high-conductivity limit simply scales with Rm (Bräuer & Krause 1974). The same is true for this quantity in the case of AMRI. From Fig. 10 the relation is

$$q = \varepsilon_{mag} (Rm - Rm_{crit}) \quad (20)$$

with $\varepsilon_{mag} \simeq 6 \cdot 10^{-4}$. It should thus be possible that the energy of the magnetic fluctuations reaches the order of the magnetic background field. The relation (20) can also be written as $q \propto \varepsilon_{mag} \Omega / \omega_\eta$. The saturation of the relation (20) for large magnetic Reynolds numbers, however, is not yet known. A possible form of the relation might be $q \propto \Omega_A^2 / \Omega^2$.

Figure 10 also shows that the magnetic energy always

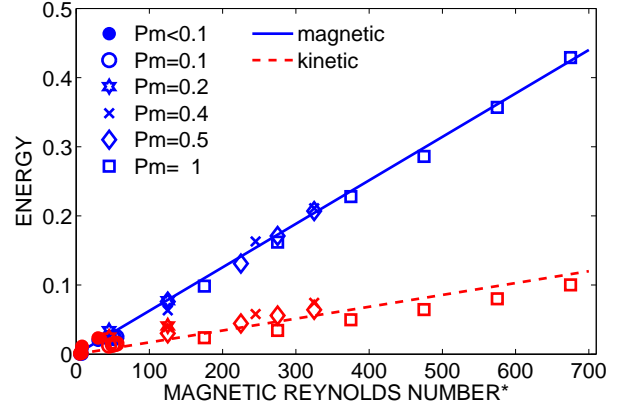


Figure 10. The magnetic (solid) and the kinetic (dashed) energies of AMRI for various magnetic Prandtl numbers vs. the magnetic Reynolds numbers. $Re = 1000$, $Ha = 75 \dots 200$, $\mu_\Omega = 0.26$, $Pm = 0.05 \dots 1$.

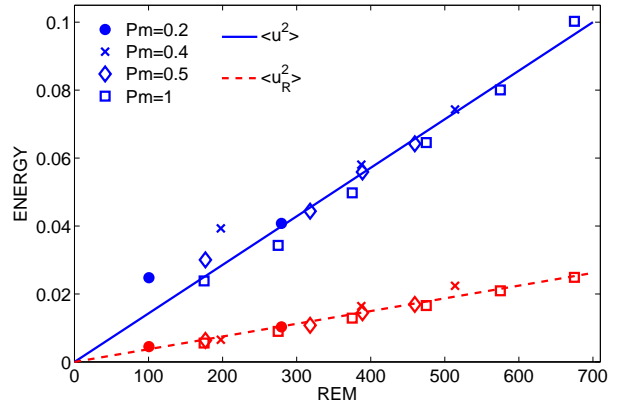


Figure 11. The kinetic energy (solid) and its part in the radial direction (dashed) of the AMRI perturbations for various Pm vs. the modified magnetic Reynolds number \bar{Rm} . $Ha = 75 \dots 200$, $\mu_\Omega = 0.26$.

dominates the kinetic energy of the fluctuations. One may speculate that the factor of four which arises here also appears in the ratio of the resulting eddy viscosity and the chemical diffusivity (see below). According to Fig. 11 the kinetic energy for various magnetic Prandtl numbers vs. the modified Reynolds number $\bar{Rm} = Rm / \sqrt{Pm} = \Omega_{in} R_{in}^2 / \bar{\eta}$ with $\bar{\eta} = \sqrt{\nu \eta}$ provides the linear relation

$$\frac{\mu_0 \rho \langle u^2 \rangle}{B_{in}^2} = \varepsilon_{kin} (\bar{Rm} - \bar{Rm}_{crit}) \quad (21)$$

with $\varepsilon_{kin} \simeq 1.4 \cdot 10^{-4}$. Hence,

$$\frac{u_{rms}}{\Omega_{in} R_{in}} \simeq 0.012 \bar{\Lambda}^{0.5} \quad (22)$$

with the modified Elsasser number

$$\bar{\Lambda} = \frac{B_{in}^2}{\mu_0 \rho \Omega \bar{\eta}}, \quad (23)$$

which does *not* depend on the size of the container. The appearance of the molecular viscosity in the expression of the kinetic energy might have strong consequences for the value of the kinetic energy. As the ratio of the magnetic

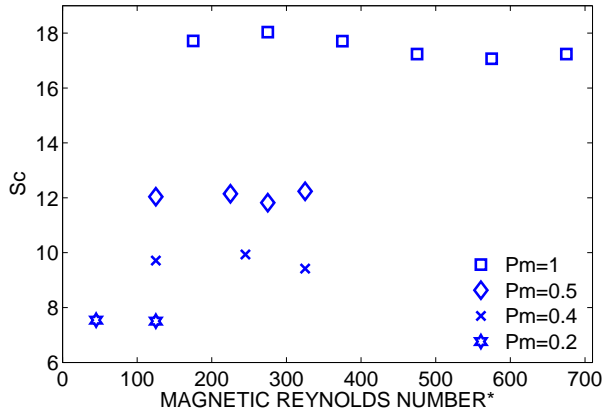


Figure 12. The proxy (25) of the turbulent Schmidt number for various magnetic Prandtl numbers and for $\mu_\Omega = 0.26$ does not depend on the magnetic Reynolds number but decreases as \sqrt{Pm} .

and kinetic energies scales with \sqrt{Pm} it should be possible, for small magnetic Prandtl numbers, that the kinetic energy even dominates the magnetic energy. For not too small Pm , however, it is clear that the AMRI provides higher values of the viscosity than for the diffusivity of chemicals. The angular momentum transport is dominated by the magnetic energy while magnetic fluctuations do not contribute to the diffusion of thermal energy and/or the mixing of chemicals (Vainshtein & Kichatinov 1983). The different scaling of the magnetic and kinetic energies has consequences for their ratio $\epsilon = \langle b^2 \rangle / \mu_0 \rho \langle u^2 \rangle$, which obviously scales as \sqrt{Pm} . The magnetic energy only dominates for magnetic Prandtl numbers of order unity or larger. Consequently, the turbulent Schmidt number

$$Sc = \frac{\nu_T}{D_T} \simeq \epsilon_R \quad (24)$$

should also scale with \sqrt{Pm} . Here ϵ_R is formed with the radial velocity components (also given in Fig. (11)), i.e.

$$\epsilon_R = \frac{\langle b^2 \rangle}{\mu_0 \rho \langle u_R^2 \rangle}, \quad (25)$$

as only the radial turbulent intensity is responsible for the radial mixing of chemicals. Figure 12 demonstrates that indeed the turbulent Schmidt number on the basis of AMRI strongly exceeds unity, but decreases with \sqrt{Pm} for small Pm . Note, however, that for very small magnetic Prandtl number it cannot become smaller than 0.4 (Yousef et al. 2003). In media with small magnetic Prandtl number the angular momentum transport and the mixing of chemicals by AMRI are of the same intensity. Both effects only stop when the regime of rigid rotation is reached. As long as the differential rotation is strong enough the mixing of chemicals is also strong. It might be, however, that the inclusion of the ‘negative’ buoyancy by the stable stratification of real stellar cores only reduces the mixing rather than the angular momentum transport and the Schmidt number is not reduced too much by the small magnetic Prandtl number (Kitchatinov & Brandenburg 2012).

REFERENCES

- Bräuer H.J., Krause F., 1974, *Astron. Nachr.*, 295, 223
 Deville M.O., Fischer P.F., Mund E.H., 2002, *High-Order Methods for Incompressible Fluid Flow*. Cambridge University Press, Cambridge
 Eggenberger P., Montalbán J., Miglio A., 2012, *A&A*, 544, L4
 Gellert M., Rüdiger G., Fournier A., 2007, *Astron. Nachr.*, 328, 1162
 Hollerbach R., Teeluck V., Rüdiger G., 2010, *Physical Review Letters*, 104, 44502
 Kirillov O.N., Stefani F., Fukumoto Y., 2012, *ApJ*, 756, 83
 Kitchatinov L.L., Rüdiger G., 2010, *A&A*, 513, L1
 Kitchatinov L.L., Brandenburg, A., 2012, *Astron. Nachr.*, 333, 230
 Michael D., 1954, *Mathematica* 1, 54
 Rüdiger G., Kitchatinov L.L., 1996, *ApJ*, 466, 1078
 Rüdiger G., Hollerbach R., 2004, *The Magnetic Universe*. Wiley-VCH, Berlin
 Rüdiger G. et al., 2007, *MNRAS*, 377, 1481
 Rüdiger G. et al., 2012, *ApJ*, 755, 181
 Seilmayer M. et al., 2012, *Physical Review Letters*, 108, 244501
 Stefani F. et al., 2009, *Physical Review E*, 80, 066303
 Tayler R.J., 1957, *Proceedings of the Physical Society, Section B*, 70, 31
 Tayler R.J., 1973, *MNRAS*, 161, 365
 Vainshtein S.I., Kichatinov L.L., 1983, *Geophysical Astrophysical Fluid Dyn.*, 24, 273
 Vandakurov Y.V., 1972, *SvA*, 16, 265
 Velikhov E.P., 1959, *Sov. Phys. JETP*, 9, 995

This paper has been typeset from a \LaTeX file prepared by the author.